FACTA UNIVERSITATIS
Series: **Mechanical Engineering** Vol. 20, Nº 3, 2022, pp. 553 - 560
https://doi.org/10.22190/FUME220730040H

Original scientific paper

BENDING FATIGUE BEHAVIOR OF AG NANOWIRE/CU THIN-FILM HYBRID INTERCONNECTS FOR WEARABLE ELECTRONICS

Byungil Hwang[1], Yurim Han[1], Paolo Matteini[2]

[1]School of Integrative Engineering, Chung-Ang University, Republic of Korea
[2]Institute of Applied Physics "Nello Carrara", National Research Council, Italy

Abstract. *Enhancing the mechanical reliability of metal interconnects is important for achieving highly reliable flexible/wearable electronic devices. In this study, Ag nanowire and Cu thin-film hybrid interconnects were explored as a novel concept to enhance mechanical reliability under bending fatigue. Bending fatigue tests were conducted on the Cu thin films and Cu/Ag nanowire/polyimide (CAP) interconnects. The increase in resistance was larger for the Cu thin films than for the CAP. The single-component Cu electrodes showed multiple crack initiation and propagation due to bending strain, which degraded the electrical conductivity. In CAP, however, no long-range cracks were observed, even after 300,000 cycles of bending, although a wavy structure was observed, probably due to the delamination of the Ag nanowires under repeated bending. Our study confirms that flexible Ag nanowire and metal thin-film hybrids can enhance the mechanical reliability of metal thin-film interconnects under bending fatigue.*

Key words: *Thin film, Stability, Bending, Ag Nanowire, Flexibility*

1. INTRODUCTION

With the progress in the field of flexible/wearable electronics, there are increasing demands for flexible interconnects that are reliable under repeated bending deformation [1-7]. Metal thin films are the most commonly used materials for flexible interconnects due to their high electrical conductivity and compliant nature [8, 9]. Metal electrodes can work as flexible electrodes for devices that undergo strain under the elastic limit. However, actual electronic devices can undergo more than 300,000 cycles of bending deformation in their lifetime of operation [10]. This causes fatigue damage on the metal thin film even though the strain is under the elastic limit. Schwaiger et al. reported that the dislocation

Received: July 30, 2022 / Accepted September 28, 2022
Corresponding author: Byungil Hwang
School of Integrative Engineering, Chung-Ang University, 84 Heukseok-Ro, Dongjak-Gu, Seoul 06974, Republic of Korea
E-mail: bihwang@cau.ac.kr

accumulation at the interface between a metal thin film and polymer substrate occurs under many cycles of bending, which leads to the formation of voids at the interfaces [11, 12]. With repeated bending, such accumulated voids create protrusions at the surface of the metal thin film, where the imposed stress is localized, resulting in the failure of the electrodes. The cracks block the electrical current flow, which can cause malfunctioning of the devices using the metal thin-film electrodes.

To enhance mechanical reliability, several alternatives have been studied, including graphene, carbon nanotube, metal nanowire, metal/graphene hybrid system, or holey metal thin-film electrodes [9, 13, 14]. Graphene, carbon nanotube, and metal nanowire are highly flexible and transparent in the visible range, but their conductivity is insufficient for interconnects. Metal-graphene hybrid systems have shown better reliability under repeated bending deformation, but the scale-up of the electrode is limited due to the size of graphene [15]. In addition, the fabrication process using multiple transfers is complex, which significantly increases the processing cost. The mechanical reliability of metal interconnects is enhanced by forming holes on the metal thin films [16]. Crack propagation is blocked by the holes, which reduces long-range crack densities on metal thin films during repeated deformations. However, a complex patterning process is required to form the holes, which increases the fabrication costs.

To overcome the limitations of the previously reported technologies, hybrid systems of flexible materials and metal thin films are a promising option. By integrating a flexible material (which can be simply formed on the polymer substrates) with a metal thin film, both high conductivity and flexibility can be achieved. Considering this, in this study, Ag nanowire and Cu thin-film hybrid interconnects were investigated. Ag nanowires are highly flexible because of their nanoscale dimensions and network structure; in addition, their mass production is possible via the polyol reduction process [17-23]. The coating process is a very simple solution-based process using a spray or doctor blade system. In this study, Ag nanowires were coated on polyimide (PI) substrates using a doctor blade. Cu thin films were deposited on the Ag nanowire/PI samples via a magnetron sputtering system. The reliability of the Cu/Ag nanowire/PI (CAP) interconnects was examined using a bending fatigue tester. Our study showed that the CAP had better reliability than Cu thin-film interconnects.

2. Materials and Methods

2.1. Sample preparation and characterization

For this study, 0.1 wt% Ag nanowire suspension in ethanol was purchased from SG Flexio (South Korea) and used as received. Fig. 1 shows the schematic illustration of fabrication process of CAP interconnects. First, A 125-μm-thick PI substrate (Dupont, Kepton E) was sequentially cleaned with IPA, ethanol, and DI water in an ultrasonic bath. Each cleaning step was carried out for 5 min. Next, Ag nanowires were coated on the PI substrate using a Mayer bar (#RD 6). Third, the Ag nanowire networks were air-dried at 80 °C for 10 min using a hot plate to evaporate a remaining solvent. Lastly, a Cu thin film was deposited on the PI substrate using DC magnetron sputtering at 100 W at room temperature for 15 min. Thickness of Cu thin film was ~400 nm. The microstructures of CAP and Cu thin film were analyzed using field-emission scanning electron microscopy (FE-SEM, SIGMA, Carl Zeiss). X-ray diffraction (New D8-Advance, Bruker-AXS, USA)

was used to analyze the crystallographic orientation. Cu Kα (λ = 0.154 nm) radiation was used for XRD analysis in the 2θ range between 30º and 100º.

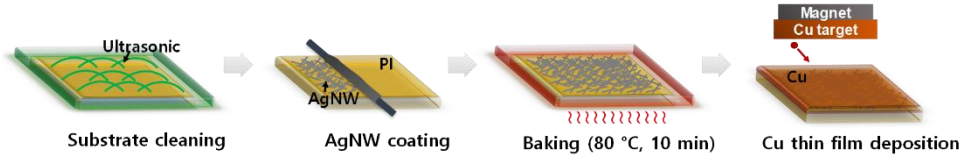

Fig. 1 Schematic illustration of a fabrication process of CAP film

2.2. Cyclic bending fatigue test

Bending fatigue tests were conducted using a cyclic bending fatigue tester (South Korea, CK Trading Co. Ltd.), which can measure electrical resistance in situ with a resolution of ~0.003 Ω. Fig. 2 presents the mechanism of a bending fatigue tester. The samples were mounted between the two horizontal plates, and both ends of the samples were fixed to the plates with screw bolts. The resistance was measured in situ across the two ends of the samples that were in contact with the metal pads. The value of the imposed strain was calculated using $\varepsilon = y/2r$, where ε, y, and r are the imposed strain value, the distance from the neutral axis, and the radius, respectively. By adjusting the distance between the two plates, the value of r varies, which results in the change of bending strain imposed on the samples. During bending tests, the lower plates move forward and backward repeatedly in the horizontal direction, thereby imposing many cycles of bending. By measuring the resistance change in situ during the bending tests, the crack evolution in the samples can be evaluated.

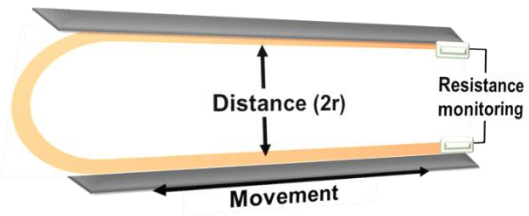

Fig. 2 Schematic of a bending fatigue testing system

3. Results

3.1. Crystallographic analysis using XRD

Fig. 3 shows XRD patterns of single Cu and CAP films. Similar XRD patterns were observed for both Cu and CAP films, where typical (111) peaks at 43.71º and 43.69º were strongly indicated with weak (200) texture at 50.44º and 50.28º, respectively as shown in Fig. 3a,b. The observed peaks at diffraction angle below 40º was noise as can be seen in XRD pattern of PI in Fig. 3c. There were no peak shifts at each peak, which confirmed Cu

and CAP films had the same texture. In addition, the grain size is calculated according to the Scherrer equation:

$$D = \frac{K \cdot \lambda}{\beta \cdot \cos\theta} \tag{1}$$

where D, K, λ, β and θ are the grain size, the shape factor, the wavelength, the full width at half maximum (FWHM), and the diffraction angle, respectively. Here, K is 0.9 for typical Cu and λ is 0.154 nm. The FWHM was evaluated for the (111) peak of Cu and CAP films, which were 0.56 and 0.55, respectively. With those parameters, the grain sizes are calculated as 15.3 nm and 15.5 nm for Cu and CAP films, respectively. Therefore, the crystallinity of Cu and CAP films was confirmed to be similar; artifacts that can be resulted from the different crystallinity is minuscule, especially for understanding of deformation behavior under bending fatigue.

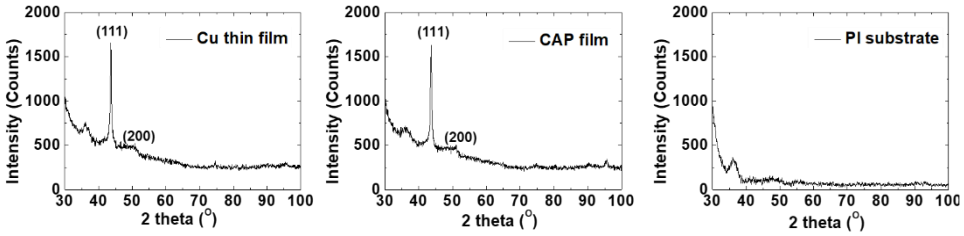

Fig. 3 XRD analysis results of (a) Cu thin film, (b) CAP film, and (c) polyimide substrate

3.2. Cyclic bending fatigue test results

Fig. 4a shows the resistance change of CAP and Cu thin film as a function of bending cycles under bending radius of 3 mm. The y-axis represents the normalized resistance change calculated by dividing the resistance gap between the measured resistance and the initial resistance value with the initial resistance value, and the x-axis represents the number of bending cycles. To confirm the reliability under severe conditions, up to 300,000 cycles bending cycles were imposed on the samples. For the Cu thin film, the resistance increased rapidly up to 40,000 cycles of bending and then showed a transient point, where a slower increase in resistance was observed until the end of the bending cycles. At the end of the bending tests, the resistance increased by 300% compared to the initial resistance. Meanwhile, the resistance of CAP increased faster than that of the Cu thin films in the initial period of the bending cycles. The transient point, where the trend of resistance increase changed from rapid increase to gradual increase, was observed at 20,000 cycles of bending, which is smaller than that observed for Cu thin films (Fig. 2b). However, the amount of resistance increase at the transient point was smaller for the CAP than for the Cu thin films. A ~113% increase in resistance was observed for the CAP film at the transient point, whereas a ~151% increase in resistance was observed for the Cu thin films. In addition, the increase in resistance at the end of the bending cycles was smaller for the CAP than for the Cu thin films. These results confirm that CAP is more reliable under large numbers of bending cycles compared to single Cu thin films.

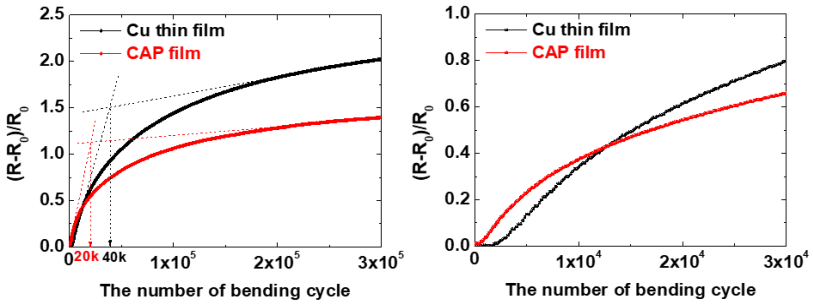

Fig. 4 (a) Normalized resistance changes in CAP and Cu thin films as a function of the number of bending cycles, and (b) replotted results in the early stage of bending cycles, 30,000 cycles

To investigate the mechanism of enhanced reliability of CAP under bending fatigue, SEM images were taken for the CAP and Cu thin films after imposing 300,000 cycles of bending, as shown in Fig. 3. The Cu thin films showed multiple cracks on the entire film area. The enlarged image of the cracks shows extrusion formation (Fig. 3a). On the contrary, there was no clear crack formation in the CAP, as seen in Fig. 3b. Wavy traces were observed in the CAP after imposing 300,000 cycles of bending (the lower inset of Fig. 3b).

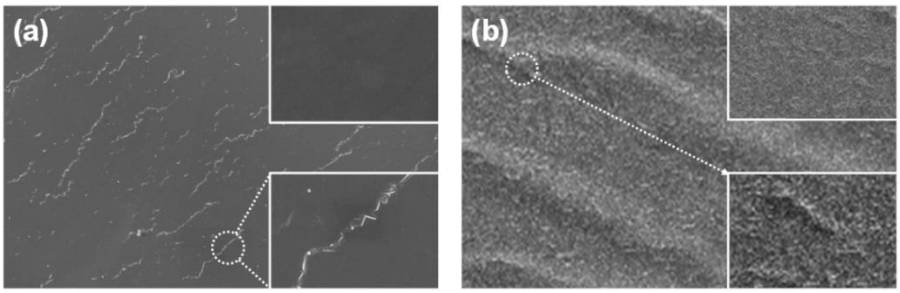

Fig. 5 SEM images of (a) Cu thin films and (b) CAP after 300,000 bending cycles

4. Discussion

The enhanced mechanical reliability for CAP film can be attributed to two factors: (1) stress relaxation by forming wavy structure and (2) reduced strain by the relocation of neutral plain due to the addition of Ag nanowires. As shown in the upper inset of Fig. 3a, Cu thin films showed no cracks before bending. Under repeated bending, dislocation accumulation occurred at the interface between the thin film and substrate (Fig. 6a), which resulted in extrusion formation (the lower inset of Fig. 3a). With the progression of bending fatigue, the stress localized on the extrusion, which led to the generation of cracks (Fig. 6a). The crack formation degraded the electrical conductivity of the metal thin films. As shown in the upper inset of Fig. 3b, the CAP showed no wavy structure before bending. The wavy structure could be attributed to the delamination of the thin film from the

substrate owing to the weak adhesion of Ag nanowires with the PI substrate (Fig. 6b). In the CAP, Cu was attached to the substrate with relatively high bonding forces, whereas the Ag nanowires were weakly attached by physical bonding forces, such as van der Waals or electrostatic forces. Under the cyclic bending, the weak interface resulted from Ag nanowires can cause delamination or interfacial sliding of thin films, forming the wavy structure. Such wavy structure might have induced micro-cracks, which were not observed in the SEM images because the cracks were closed in the no-strain state (Fig. 6b). Because of the micro-cracks, an increase in resistance was observed in the CAP. However, there were no long-range cracks in the CAP, unlike in the Cu thin films; thus, the increase in resistance was smaller for the CAP than for the Cu thin films. In the initial stage of bending, however, the CAP underwent the deformation by forming wavy structure, which was earlier than the point where the crack formation and propagation of single Cu thin films occurred. During which, short range of micro cracks can be formed at the wavy structure of CAP; thus, the resistance can be slightly increased. The micro cracks are difficult to observe in SEM or TEM because the cracks are closed. Thus, the resistance increase of CAP in the initial stage was higher than those of single Cu thin films.

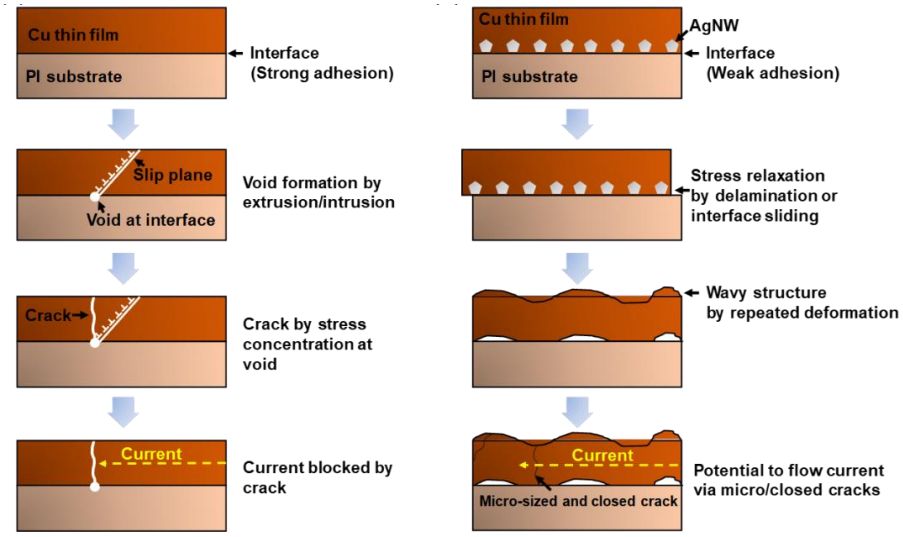

Fig. 6 Illustration of failure mechanism of (a) Cu and (b) CAP films under cyclic bending

Second, the relocation of neutral plane position by the addition of Ag nanowires can vary the strain imposed on the metal thin film as shown in Fig. 7. The imposed bending strain is calculated by the equation:

$$S = \frac{\sum_{i=0}^{n} B_i (y_{i+1}^2 - y_i^2)}{2\sum_{i=0}^{n} B_i (y_{i+1} - y_i)} \tag{2}$$

where S, B and $y_{(i+1)} - y_1$ (Δy) are the neutral plane position, the biaxial modulus and the thickness of each layer, respectively [14, 24]. The biaxial modulus, B, is calculated by the equation:

$$B = \frac{E}{1-\nu} \tag{3}$$

where E is the elastic modulus and ν is Poisson's ratio. Table 1 shows parameters used for the calculation of neutral plane position. With those parameters, the calculated neutral positions were 69.3 and 71.2 μm for the Cu and CAP films, respectively. Therefore, the imposed strains on the Cu and CAP films are calculated as 2.8% and 2.7%, respectively. The difference between the calculated imposed strain values was ~0.1%. Although the strain value itself is not significant; this small value can make a reasonable change in the results of cyclic bending tests where more than 300,000 cycles of bending is imposed.

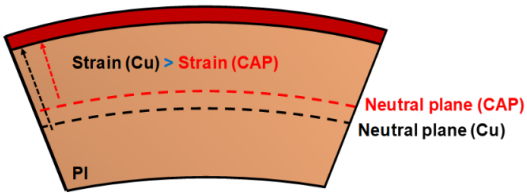

Fig. 7 Illustration of change in imposed strain on metal thin film by the relocation of neutral plane position

5. Conclusion

In this study, Cu/Ag nanowire/PI (CAP) interconnects were explored as a novel concept to improve the mechanical reliability of single-component Cu electrodes. Bending fatigue tests were conducted for the CAP and Cu thin films while monitoring the resistance in situ. The resistance change reflected the crack or failure evolution in the thin films during the bending tests. The results of the bending fatigue test showed that the CAP exhibited better mechanical reliability compared to the Cu thin films, with a lower increase in resistance after 300,000 cycles of bending. Microstructural analysis through SEM showed a high density of long-range cracks in Cu thin films after imposing 300,000 cycles of bending; CAP showed no such long-range cracks but exhibited a wavy structure, probably due to the delamination of Ag nanowires by the bending strain. Our study confirms that flexible Ag nanowires and metal thin-films hybrids can enhance the mechanical reliability of metal thin-film interconnects under bending fatigue.

Acknowledgement: *This work was supported by a National Research Foundation of Korea (NRF) grant funded by the Korean government (MSIT) (No. NRF-2019K1A3A1A25000230). This research was supported by the Chung-Ang University Graduate Research Scholarship in 2022.*

References

1. Hwang, B., An, Y., Lee, H., Lee, E., Becker, S., Kim, Y.-H., Kim, H., 2017, *Highly flexible and transparent ag nanowire electrode encapsulated with ultra-thin al2o3: Thermal, ambient, and mechanical stabilities*, Scientific Reports, 7(1), 41336.
2. Kim, D., Kim, S.-H., Kim, J.H., Lee, J.-C., Ahn, J.-P., Kim, S.W., 2017, *Failure criterion of silver nanowire electrodes on a polymer substrate for highly flexible devices*, Scientific Reports, 7(1), 45903.

3. Mastrogiannakis, I., Vosniakos, G.-C., 2020, *Exploring structural design of the francis hydro-turbine blades using composite materials*, Facta Universitatis, Series: Mechanical Engineering, 18(1), pp. 43-55.
4. Sae-Long, W., Limkatanyu, S., Sukontasukkul, P., Damrongwiriyanupap, N., Rungamornrat, J., Prachasaree, W., 2021, *Fourth-order strain gradient bar-substrate model with nonlocal and surface effects for the analysis of nanowires embedded in substrate media*, Facta Universitatis, Series: Mechanical Engineering, 19(4), pp. 657-680.
5. Qaiser, N., Damdam, A.N., Khan, S.M., Bunaiyan, S., Hussain, M.M., 2021, *Design criteria for horseshoe and spiral-based interconnects for highly stretchable electronic devices*, Advanced Functional Materials, 31(7), 2007445.
6. Ha, H.-B., Lee, B.H., Qaiser, N., Seo, Y., Kim, J., Koo, J.M., Hwang, B., 2022, *Highly reliable anisotropic interconnection system fabricated using cu/sn-soldered microdumbbell arrays and polyimide films for application to flexible electronics*, Intermetallics, 144, 107535.
7. Qaiser, N., Damdam, A.N., Khan, S.M., Elatab, N., Hussain, M.M., 2021, *Mechanical reliability of self-similar serpentine interconnect for fracture-free stretchable electronic devices*, Journal of Applied Physics, 130(1), 014902.
8. Park, M., Kim, W., Hwang, B., Han, S.M., 2019, *Effect of varying the density of ag nanowire networks on their reliability during bending fatigue*, Scripta Materialia, 161, pp. 70-73.
9. Kim, T., Canlier, A., Kim, G.H., Choi, J., Park, M., Han, S.M., 2013, *Electrostatic spray deposition of highly transparent silver nanowire electrode on flexible substrate*, ACS Applied Materials & Interfaces, 5(3), pp. 788-794.
10. Hwang, B., Shin, H.A.S., Kim, T., Joo, Y.C., Han, S.M., 2014, *Highly reliable ag nanowire flexible transparent electrode with mechanically welded junctions*, Small, 10(16), pp. 3397-3404.
11. Schwaiger, R., Kraft, O., 1999, *High cycle fatigue of thin silver films investigated by dynamic microbeam deflection*, Scripta Materialia, 41(8), pp. 823-829.
12. Schwaiger, R., Kraft, O., 2003, *Size effects in the fatigue behavior of thin ag films*, Acta Materialia, 51(1), pp. 195-206.
13. Hwang, B., Park, M., Kim, T., Han, S., 2016, *Effect of rgo deposition on chemical and mechanical reliability of ag nanowire flexible transparent electrode*, RSC Advances, 6(71), pp. 67389-67395.
14. Lee, C., Kim, H., Hwang, B., 2019, *Fracture behavior of metal oxide/silver nanowire composite electrodes under cyclic bending*, Journal of Alloys and Compounds, 773, pp. 361-366.
15. Hwang, B., Kim, W., Kim, J., Lee, S., Lim, S., Kim, S., Oh, S.H., Ryu, S., Han, S.M., 2017, *Role of graphene in reducing fatigue damage in cu/gr nanolayered composite*, Nano Letters, 17(8), pp. 4740-4745.
16. Kim, B.-J., Cho, Y., Jung, M.-S., Shin, H.-A.-S., Moon, M.-W., Han, H.N., Nam, K.T., Joo, Y.-C., Choi, I.-S., 2012, *Fatigue-free, electrically reliable copper electrode with nanohole array*, Small, 8(21), pp. 3300-3306.
17. Hu, L., Kim, H.S., Lee, J.-Y., Peumans, P., Cui, Y., 2010, *Scalable coating and properties of transparent, flexible, silver nanowire electrodes*, ACS Nano, 4(5), pp. 2955-2963.
18. Lee, J., Lee, I., Kim, T.S., Lee, J.Y., 2013, *Efficient welding of silver nanowire networks without post-processing*, Small, 9(17), pp. 2887-2894.
19. Liu, C.-H., Yu, X., 2011, *Silver nanowire-based transparent, flexible, and conductive thin film*, Nanoscale Research Letters, 6(1), pp. 1-8.
20. Liu, R., Tan, M., Zhang, X., Xu, L., Chen, J., Chen, Y., Tang, X., Wan, L., 2018, *Solution-processed composite electrodes composed of silver nanowires and aluminum-doped zinc oxide nanoparticles for thin-film solar cells applications*, Solar Energy Materials and Solar Cells, 174, pp. 584-592.
21. Zeng, X.Y., Zhang, Q.K., Yu, R.M., Lu, C.Z., 2010, *A new transparent conductor: Silver nanowire film buried at the surface of a transparent polymer*, Advanced Materials, 22(40), pp. 4484-4488.
22. Zhang, D., Ryu, K., Liu, X., Polikarpov, E., Ly, J., Tompson, M.E., Zhou, C., 2006, *Transparent, conductive, and flexible carbon nanotube films and their application in organic light-emitting diodes*, Nano letters, 6(9), pp. 1880-1886.
23. Yang, L., Zhang, T., Zhou, H., Price, S.C., Wiley, B.J., You, W., 2011, *Solution-processed flexible polymer solar cells with silver nanowire electrodes*, ACS Applied Materials & Interfaces, 3(10), pp. 4075-4084.
24. Jing, H., Gou, M., Song, L., 2021, *Research on bending fatigue properties of reinforced macadam foundation*, Tehnički vjesnik, 28(4), pp. 1211-1220.